A PULSE RADIOLYSIS STUDY OF FREE RADICALS FORMED BY ONE ELECTRON OXIDATION OF THE ANTIMALARIAL DRUG PYRONARIDINE.

Fyaz M. D. Ismail[1], Michael G.B.Drew[2], Suppiah Navaratnam[3,4] and Roger H. Bisby[3]*

[1]School of Pharmacy and Biomolecular Sciences, Liverpool John Moores University, Liverpool L3 3AF, UK

[2]Department of Chemistry, University of Reading, Reading RG6 6AD, UK

[3]Biomedical Sciences Research Institute, University of Salford, Salford M5 4WT, UK

[4]Free Radical Research Facility, STFC Daresbury Laboratory, Warrington, WA4 4AD, UK.

*Author for correspondence, email r.h.bisby@salford.ac.uk

ABSTRACT

Free radicals from one-electron oxidation of the antimalarial drug pyronaridine have been studied by pulse radiolysis. The results show that pyronaridine is readily oxidised to an intermediate semiiminoquine radical by inorganic and organic free radicals, including those derived from tryptophan and acetaminophen. The pyronaridine radical is rapidly reduced by both ascorbate and caffeic acid. The results indicate that the one-electron reduction potential of the pyronaridine radical at neutral pH lies between those of acetaminophen (707 mV) and caffeic acid (534 mV). The pyronaridine radical decays by a second order process which DFT calculations (UB3LYP/6-31+G*) suggest is a disproportionation reaction. Important calculated dimensions of pyronaridine, its phenoxyl and aminyl radical as well as the iminoquinone are presented.

KEYWORDS:- Pyronaridine, free radical, pulse radiolysis, oxidation, DFT antimalarial

INTRODUCTION

The massive problem of endemic and drug-resistant malaria in tropical countries, especially that due to potentially fatal infections with *Plasmodium falciparum*, has led to the development of a wide range of antimalarial drugs [1]. Pyronaridine (Figure 1) was introduced as an antimalarial agent in the 1970's as a development of the existing antimalarial drug amodiaquine [2,3]. Although an effective antimalarial agent, amodiaquine has the potential to induce potentially fatal hepatotoxicity [4] and has now been withdrawn from use, except in the treatment of acute and resistant infections. Toxicity of amodiaquine results from oxidation of the aminophenol function, probably through the intermediate formation of the semiiminoquinone radical [5], and formation of a reactive iminoquinone [6-9]. In comparison, pyronaridine shows less clinical toxicity but retains some of the biochemical properties associated with amodiaquine toxicity such as oxidation by peroxidases, iminoquinone formation, glutathione depletion and cytotoxicity [6]. These reactions of the aminophenol function in antimalarial drugs reflect the well known toxicity of the same group within acetaminophen (N-acetylaminophenol, APAP) [10]. The pyronaridine molecule is normally formulated for clinical use as the tetraphosphate and Figure 1 indicates the pK_a values for proton loss at the various sites in the molecule [11]. Pyronaridine is of particular interest since it has been reported to be active against multidrug-resistant strains of *Plasmodium* [12], inhibits *Plasmodium falciparum* topoisomerase II [13] and is being evaluated for world wide prophylactic use against all strains (drug resistant and sensitive) of malaria [1].

{FIGURE 1}

The propensity for oxidation of the aminophenol function in both amodiaquine and pyronaridine is involved not only in toxic side effects but may also be involved in their modes of antimalarial action. In the intra-erythrocytic stage the malaria parasite degrades haemoglobin and utilises the released amino acids for its own catabolism [14]. The heme that is simultaneously released is potentially toxic to the parasite through reactions that induce oxidative stress and contribute to the pathophysiology of fatal cerebral malaria [15]. Biocrystallization of the free heme, which may be a spontaneous or enzymically promoted process [16], produces redox inactive β-hematin, also known as hemozoin or malaria pigment [17]. This eliminates oxidative stress due to free heme and allows the parasite to survive. Compounds that inhibit heme biocrystallization also possess antimalarial activity [18]. Recent results indicate that pyronaridine forms a complex with hematin that inhibits further biocrystallization [19]. This is now considered to be the mode of action rather than inhibition of parasite topoisomerase [13]. Such interactions appear to depend on a slipped offset interaction [3, 18] rather than the previously assumed π–π interactions between drug and hematin, with the drug acting as a partial electron donor.

Pulse radiolysis studies have previously been used to study the redox behaviour of phenols and aminophenols and the properties of the phenoxyl and semi(imino)quinone radicals formed by one-electron oxidation [20,21]. Pulse radiolysis studies of both APAP [22] and amodiaquine [23] have been reported. The present pulse radiolysis study has been undertaken to assess the reactivity and reduction potential of the intermediate free radical formed by one-electron oxidation of pyronaridine.

MATERIALS AND METHODS

Pyronaridine tetraphosphate was a gift from Professor D Warhurst (London School of Hygiene and Tropical Medicine). The model compound *N*-(4-hydroxy-3,5-*bis*(pyrrolidin-1-ylmethyl)phenyl)acetamide, SA48, was prepared by a published procedure [24]. Other chemicals used were of Analar grade and solutions were prepared in water obtained from a Millipore Milli Q unit or equivalent.

Pulse radiolysis was undertaken using the Daresbury linear accelerator with pulses of 12 MeV electrons [25]. The radiation dose was approximately 6 Gy per pulse with a pulse length of 200 ns. The solution was irradiated in a quartz capillary cell with an optical pathlength of 2.5 cm and dosimetry was performed with an air saturated solution of KSCN (10 mmol dm^{-3}).

RESULTS

1. Oxidation of pyronaridine by inorganic radicals

The oxidizing inorganic radicals $N_3^{\bullet}$ (E_o' 1.33 V [26]) and $Br_2^{-\bullet}$ (E_o' 1.66 V [26]) were produced by pulse radiolysis of N_2O-saturated solutions containing the corresponding salt:-

$$H_2O \rightsquigarrow {}^{\bullet}OH, e_{aq}^{-}, H^{\bullet}$$
$$e_{aq}^{-} + N_2O \rightarrow {}^{\bullet}OH + N_2 + OH^{-}$$
$${}^{\bullet}OH + N_3^{-} \rightarrow N_3^{\bullet} + OH^{-}$$
$${}^{\bullet}OH + 2Br^{-} \rightarrow Br_2^{-\bullet} + OH^{-}$$

In addition, the oxidizing trichloromethylperoxyl radical, $CCl_3O_2^{\bullet}$ (E_o' 1.3 V [26]), was produced in solutions saturated with N_2O/O_2 (4:1 v/v) containing acetone, propan-2-ol and CCl_4 :-

$$e_{aq}^{-} + H^{+} + (CH_3)_2CO \rightarrow (CH_3)_2{}^{\bullet}COH$$
$${}^{\bullet}OH + (CH_3)_2CHOH \rightarrow (CH_3)_2{}^{\bullet}COH + H_2O$$
$$(CH_3)_2{}^{\bullet}COH + CCl_4 \rightarrow (CH_3)_2CO + CCl_3^{\bullet} + Cl^{-} + H^{+}$$
$$CCl_3^{\bullet} + O_2 \rightarrow CCl_3O_2^{\bullet}$$

At pH < 7, both azidyl radical and dibromide radical anion reacted with pyronaridine to produce a product radical with absorption maxima in the measured difference spectrum at 540 and 630 nm (Figures 2A and 2B). The difference spectra also displayed bleaching in the region of the long wavelength absorption maximum of pyronaridine at 430 nm (Figure 2B). As the pH was increased the transient absorption spectrum resulting from oxidation by azidyl radicals (Figure 2A) was transformed to one with absorption maxima at 490 and 600 nm, with isobestic points at ca 555 and 630 nm. The transient spectra obtained by oxidation of pyronaridine by the trichloromethylperoxyl radical at pH 7.7 (Figure 2B) was very similar to that formed by reaction of azidyl radical at the same pH value. The similarity in transient absorption spectra at a particular pH value produced by the different oxidizing free

radicals indicates that reaction occurs by simple one-electron oxidation and that the shift in the spectrum with pH results from deprotonation of the radical.

{FIGURE 2}

For comparison, the transient absorption spectra obtained by one-electron oxidation of the model compound 4-amino-2,6-*bis*(1-pyrrolidinylmethyl)-phenol (SA48, Figure 1) are shown in Figure 3. The transient spectra show maxima at 450 nm at pH 6.8 and 500 nm at pH 12.8, very similar to those observed previously for APAP [22] with the change resulting from deprotonation of the phenoxyl radical at the nitrogen atom with a pK_a of 11.1. Second order rate constants for reaction of oxidizing free radicals with pyronaridine and related compounds are shown in Table 1. Azidyl radicals were found to react with pyronaridine, amodiaquine, APAP and SA48 at neutral pH with rate constants in excess of 10^9 dm^3 mol^{-1} s^{-1}, close to the diffusion controlled limit and consistent with the high reduction potential for $N_3^{\bullet}$. In alkaline solution, the rate constants all increase due to deprotonation of the phenolic group (pK_a ca 10). However, measurements with pyronaridine were limited by it being virtually insoluble at pH >10. Deprotonation of the pyrrolidine groups in pyronaridine and SA28 appear to have little effect on the rate of oxidation by the azidyl radical. At neutral pH, the second order rate constant for reaction of dibromide radical anion decreases by two orders of magnitude in the order pyronaridine > amodiaquine > APAP and is taken to reflect the both influence of the positively charged pyrrolidine groups and the lower reduction potentials for amodiaquine and pyronaridine compared with APAP (see below). The electrophilic trichloromethylperoxyl radical ($CCl_3O_2^{\bullet}$) was also found oxidize pyronaridine very rapidly with a second order rate constant of 1.8 x 10^9 dm^3 mol^{-1} s^{-1}. These results suggest that the aminophenol moiety of pyronaridine is the principle site for reaction with oxidizing free radicals.

{FIGURE 3}
{TABLE 1}

2. Free radical interactions between pyronaridine and organic compounds

In aqueous solution at neutral pH, tryptophan was oxidised to the neutral indolyl radical (λ_{max} 520 nm) by azidyl radicals. The indolyl radical from tryptophan is relatively oxidising (E_o' 1.015 V [27]) and in the presence of pyronaridine was found to react, as shown by the formation of the characteristic 640 nm absorption of the pyronaridine radical at neutral pH as illustrated in Figure 4.

$$N_3^{\bullet} + TrpH \rightarrow Trp^{\bullet} + N_3^{-} + H^{+}$$
$$Trp^{\bullet} + \text{Pyronaridine-H} \rightarrow TrpH + [\text{Pyronaridine}]^{\bullet}$$

The second order rate constant for oxidation of pyronaridine by tryptophanyl radicals was found to be (8.0 ± 0.4) x 10^7 dm^3 mol^{-1} s^{-1} from the second order plot in the inset to Figure 4. The lower rate constant by over an order of magnitude compared with that determined with the inorganic radicals described above is due to the comparatively lower reduction potential of the tryptophanyl radical. The semiiminoquinone free radical from APAP (E_o' 707 mV [22]) was also found to

oxidise pyronaridine to the free radical with an apparent second order rate constant of ~ 10^8 dm^3 mol^{-1} s^{-1} as illustrated in Figure 5.

{FIGURE 4}
{FIGURE 5}

Ascorbate is highly reducing with E_o' ($Asc^{\bullet-}$, $H^+/AscH^-$) 300 mV [20]. Accordingly in solutions containing pyronaridine and lower concentrations of ascorbate, the absorption at 640 nm of the pyronaridine radical formed by oxidation with azidyl radical at neutral pH was found to decay exponentially with first order rates increasing with ascorbate concentration as illustrated in Figure 6. The inset to Figure 6 shows the second order plot giving a second order rate constant of (1.4 ± 0.1) x 10^7 dm^3 mol^{-1} s^{-1}. Caffeic acid (E_o' 534 mV [28]) was similarly found to reduce the pyronaridine radical with a second order rate constant of (5.6 ± 0.4) x 10^6 dm^3 mol^{-1} s^{-1}.

{FIGURE 6}

These free radical interactions between species with the know reduction potentials demonstrate that the one electron reduction potential of the pyronaridine radical at neutral pH lies between that of APAP (707 mV) and caffeic acid (534 mV). It was not possible to undertake the usual experiments to determine transient equilibria with redox standards at high pH (>12) [20] due to the insolubility of pyronaridine under these conditions.

3. Decay of the pyronaridine radical

The radical described above formed from the one-electron oxidation of pyronaridine was unstable and decayed on a millisecond timescale. The decay of the difference spectrum at pH 6.7 is illustrated in Figure 7. The radical peaks at 540 and 640 nm decay and are replaced by a much less intense residual absorbance peaking in the region of 550 – 600 nm. At all wavelengths the decay could be fitted to a second order process plus a residual product absorbance. The decay at 640 nm is shown in the inset to Figure 7 and gave a second order rate constant for decay ($2k_2$) of (45.2 ± 0.1) x 10^8 dm^3 mol^{-1} s^{-1}. This value is based an on an extinction coefficient of of 4,700 dm^3 mol^{-1} cm^{-1} at 640 nm, assuming quantitative oxidation of pyronaridine by azidyl radical. The observed second order decay could be explained by either a radical termination (i.e. dimerization) or a disproportionation reaction. The second possibility appears to be more consistent with steric hinderance imposed by two methylene pyrrolidinyl groups occupying both *ortho*-phenolic positions and with the residual absorption found during pulse radiolysis. In this case the product spectrum at 550 – 600 ns belongs to the iminoquinone that has been previously discussed in relation to the toxic side effects of this drug [6]. Preliminary mass spectral investigations of the products from radiolysis of a nitrous oxide saturated solution of pyronaridine containing sodium azide have revealed the formation of the quinone **3a** (Figure 8).

{FIGURE 7}

The structural details of pyronaridine and the one- and two-electron oxidised products were studied using density functional theory (DFT) methodology with the Gaussian03 program [29] to ascertain which route was thermodynamically favoured since most investigators have assumed that disproportionation is the favoured decay mode [Figure 8]. Similar combined pulse radiolytic – DFT approaches have proved successful in explaining the decay of *ortho*-substituted transient semi-iminoquinones involved in pheomelanogenesis [30].

{FIGURE 8}

For the DFT study, the input model for pyronaridine (**1**) was built in two parts. First the moiety based on the 7-chloro-2-methoxybenzo[*b*][1,5]naphthyridine heterocyclic system was attached via an NH substituent to a phenyl ring. There are only two variables, namely the C1-C2-N1-C3 and C2-N1-C3-C4 torsion angles between the aromatic rings (see Figure 9 for atom identification), and optimum values were obtained from previous calculations [31]. The second variable involves the orientations of the 4-amino-2,6-*bis*(pyrrolidin-1-ylmethyl)phenol fragment and we used experimental data from the CCDC [32]) in particular DUTTUH, DUTVAP, SOPBEE and VIMYEV which had very similar conformations. The resulting complete structural model was then fully optimised; subsequently, starting models for **2a, 2b** and **3a** were built by removing the appropriate hydrogen atom(s) from the optimised 1 and then fully optimised using the UB3LYP/6-31+G* methodology.

The enthalpies of the reactions **1** - $H^{\bullet}$ =→ **2a** and **1** – $H^{\bullet}$ →= **2b** were then studied. All entities were geometry optimised and the enthalpies of reaction were calculated as 87.1 and 87.6 kcal mol^{-1} respectively. Therefore, there is little significant difference between the energies of the phenoxyl and aminyl radicals. These values compare favourably with the free energy (76.7 kcal mol^{-1}) for the found in the related molecule 4,6-di-tert-butyl-2-tert-butylimino-semiquinone in which the phenoxyl group is also sterically hindered [33].

{FIGURE 9}

In contrast, the enthalpy of the reaction **1** - $2H^{\bullet}$ =→ **3a** was calculated as 154.97 kcal mol^{-1}. This can be compared favourably with the enthalpies for the formation of 2a + 2b, or indeed 2*2a or 2*2b which would have a combined enthalpy of ca 175 kcal mol-1. Thus the disproportionation reaction of radicals 2a and 2b to form 3a is favoured by ca 20 kcal mol^{-1}. The structures of **1, 2a, 2b** and **3a** are shown in Figure 9 with important dimensions compared in Table 2.

{TABLE 2}

It will be noted that there is, as expected, a significant change in geometry when the hydrogen on N1 is removed in **3a**. The main change is a decrease in the N1-C3 bond length by 0.136 Å which is accompanied by a change in conformation as the C2-N1-C3-C4 torsion angle changes from 139.4° to -173.6° so that the arrangement around the C3-N1 double bond is approximately planar. This increase in conjugation will cause a corresponding shift in the product absorption maximum as observed

experimentally for the iminoquinone product in Figure 7. By contrast the C1-C2-N1-C3 torsion angle changes from 145.3^{o} in 1 to 62.5^{o} in **3a** twisting further away from planarity and concomitant with a slight increase in the C2-N1 bond length which has less double bond character increasing slightly from 1.375 to 1.385 Å. The structures of the radicals **2a** and **2b** show some variations. In **2a** the C-O7 bond length is 1.257 Å, close to that for a double bond; the C-C bonds in the six-membered ring starting adjacent to the carbonyl are 1.469, 1.376,1.418, 1.421, 1.373, 1.466 Å showing that the ring loses some of its aromatic character but not all. Thus the comparable distances in the iminoquinone **3a** are 1.492, 1.349, 1.464, 1.466, 1.349, 1.493 Å. The N1-C3 in **2a** bond has slightly more double bond character than in 1 and the C2-N1-C3-C4 torsion angle increases to 172.2^{o}. By contrast the torsion angles in **2b** are almost exactly the same as in **3a**. The N1-C3 bond length at 1.343 Å retains some double bond character but is still significantly longer than the 1.296 Å found in **3a**.

There is an additional change in that in **1,** there is an intermolecular hydrogen bond between O7-H and N5 with an O7...N5 distance of 2.718Å. This is maintained in **2b** with a distance of 2.686 Å but with the removal of the hydrogen atom on O7, as in **2a** or **3a**, this distance increases to 3.361 and 3.338Å respectively. These results are consistent with conclusions drawn in Section 1 that the aminophenol moiety is the reaction site with oxidizing free radicals. Radicals such as **2a** and/or **2b** could arise through interaction of oxidizable groups with free heme(II) released during the parasite mediated catabolism of haemoglobin [34], and could contribute, in part, to the antimalarial action of compounds containing the *para*-amino phenol moiety [3].

CONCLUSIONS

Pyronaridine is readily oxidized to the radical species with a one-electron reduction potential at pH 7 for the radical species between ca 530 and 700 mV as defined by observed reactions with caffeic acid and the acetaminophen semiiminoquinone radical respectively. The result shows that pyronaridine is more readily oxidised than acetaminophen and accounts for the ease with which the drug is metabolised to toxic intermediates. The radical decays by a second order process which is suggested on the basis of spectral evidence and calculation to be a disproportionation resulting in formation of the iminoquinone that is responsible for reaction with thiols and protein conjugation *in vivo*.

SUPPLEMENTARY MATERIAL

Coordinates of the optimised structures of **1, 2a, 2b, 3a** may be found in the Supplementary Material

ACKNOWLEDGEMENTS

We thank Professor David Warhurst (London School of Tropical Medicine and Hygiene) for the kind gift of the pyronaridine sample and to Said Alizadeh-Shekalgourabi for synthesising SA48. We also thank STFC and Daresbury Laboratory

for providing access to the linear accelerator at the Synchrotron Radiation Source for pulse radiolysis studies and Dr Ruth Edge and Ms Ana Crisostomo for assistance with the experiments.

REFERENCES

1. M.Schlitzer, Antimalarial drugs – what is in use and what is in the pipeline, *Arch. Pharm. Chem. Life Sci.* **341**, 149 – 163 (2008).

2. W.Peters and B.L.Robinson, The chemotherapy of rodent malaria. 47. Studies on pyronaridine and other Mannich base antimalarials, *Ann. Trop. Med. Parasitol*. **86**, 455-465 (1992).

3. M.J.Dascombe, M.G.B.Drew, P.G.Evans and F.M.D.Ismail, Rational design strategies for the development of synthetic quinoline and acridine based antimalarials, *Front. Drug Design Disc*. **3**, 559-609 (2007).

4. A.Neftel, W.Woodtly, M.Schmid, P.G.Frick and J Fehr, Amodiaquine induced agranulocytosis and liver damage, *Br. Med. J*. **292**, 721–723 (1986).

5. J.L.Maggs. M.D.Tingle, N.R.Kitteringham and B.K.Park, Drug-protein conjugates – XIV: mechanisms of formation of protein-arylating intermediates from amodiaquine, a myelotoxin and hepatotoxin in man, *Biochem. Pharmacol*. **37**, 303-311 (1988).

6. D.J.Naisbitt, D.P.Williams, P.M.O'Neill, J.L.Maggs, D.J.Willock, M.Pirmohamed and B.K.Park, Metabolism-dependent neutrophil cytotoxicity of amodiaquine: a comparison with pyronaridine and related antimalarial drugs, *Chem. Res. Toxicol.* **11**, 1586-1595 (1998).

7. P.M.O'Neill, P.G.Bray, S.R.Hawley, S.A.Ward, B.K.Park, 4-Aminoquinolines—Past, present, and future; A chemical perspective, *Pharmacol. Ther*. **77**, 29–58 (1998).

8. P.M.O'Neill, A.Mukhtar, P.A.Stocks, L.E.Randle, S.Hindley, S.A.Ward, R.C.Storr, J.F.Bickley, I.A.O'Neil, J.L.Maggs, R.H.Hughes, P.A.Winstanley, P.G.Bray and B.K.Park, Isoquinine and related amodiaquine analogues: a new generation of improved 4-aminoquinoline antimalarials, *J. Med. Chem.* **46**, 4933-4945 (2003).

9. U.Jarva, A.Holmen, G.Gronberg, C.Masimiremba and L.Weidolf, Electrochemical generation of electrophilic drug metabolites: Characterization of amodiaquine quinoneimine and cysteinyl conjugates by MS, IR, and NMR, *Chem. Res. Toxicol.* **21**, 928-935 (2008).

10. S.D.Nelson, Mechanisms of the formation and disposition of reactive metabolites that can cause acute liver-injury, *Drug Metab. Rev*. **27**, 147-177 (1995).

11. O.A.Adegoke, C.P.Babalola, O.S.Oshitade and A.A.Famuyiwa, Determination of the physicochemical properties of pyronaridine – a new antimalarial drug, *Pak. J. Pharm.Sci.* **19**, 1-16 (2006).

12. S.A.Gamage, N.Tsepsiri, P.Wilairat, S.J.Wojcit, D.P.Figgitt, R.A.Ralph and W.A.Denny, Synthesis and in vitro evaluation of 9-anilino-3,6,-diacridines against a multidrug-resistant strain of the malaria parasite *Plasmodium falciparum*, *J. Med. Chem*. **37**, 1486-1494 (1994).

13. P.Chavalitshewinkoon, P.Wilairat, S.Gamage, W.Denny, D.Figgitt and R.Ralph, Structure-activity relationships and modes of action of 9-anilinoacridines against chloroquine-resistant Plasmodium falciparum in vitro, *Antimicrob. Agents Chemother*. **37**, 403-406 (1993).

14. G.Padmanaban and P.N.Rangarajan, Heme metabolism of Plasodium is a major antimalarial target, *Biochem. Biophys. Res. Commun.* **268**, 665-668 (2000).

15. N.H.Hunt and R.Stocker, Heme moves to center stage in cerebral malaria, *Nature Medicine* **13**, 667-669 (2007).

16. D.Jani, R.Nagarkatti, W.Beatty, R.Angel, C.Slebodnick, J.Andersen, S.Kumar and D.Rathore, HDP - A novel heme detoxification protein from the malaria parasite, *PLoS Pathog.* **4,** e1000053 (2008).

17. S.Pagola, P.W.Stephens, D.S.Bohle, A.D.Kosar and S.K.Madsen, The structure of malaria pigment beta-haematin, *Nature* **404**, 307-310 (2000).

18. M.J.Dascombe, M.G.B.Drew, H.Morris, P.Wilairat, S.Auparakkitanon, W.A.Moule, S.Alizadeh-Shekalgourabi, P.G.Evans, M.Lloyd, A.M.Dyas, P.Carr and F.M.D.Ismail, Mapping antimalarial pharmacophores as a useful tool for the rapid discovery of drugs effective in vivo: Design, construction, characterization, and pharmacology of metaquine, *J. Med. Chem*. **48**, 5423-5436 (2005).

19. S.Auparakkitanon, S.Chapoomram, K.Kuaha, T.Chirachariyavej and P.Wilairat, Targeting of hematin by the antimalarial pyronaridine, *Antimicrob. Agents Chemother.* **50,** 2197-2200 (2006).

20. S.Steenken and P.Neta, One-electron redox potentials of phenols, hydroxyl- and aminophenols and related compounds of biological interest, *J. Phys. Chem*. **86**, 3661-3667 (1982).

21. P.Neta, Radiation chemistry of quinoid compounds, in: *The Chemistry of Quinoid Compounds*, S.Patai and Z.Rappoport, (Eds), Vol II, pp. 879-898. Wiley, Chichester, (1988).

22. R.H.Bisby and N.Tabassum, Properties of the radicals formed by one-electron oxidation of acetaminophen - a pulse radiolysis study, *Biochem. Pharmacol.* **37**, 2731-2738 (1988).

23. R.H. Bisby, Reactions of a free radical intermediate in the oxidation of amodiaquine, *Biochem. Pharmacol.* **39**, 2051-2055 (1990).

24. D.M.Stout, W.L.Matier, C.Barcelon-Yang, R.D.Reynolds, B.S.Brown, Synthesis and antiarrhythmic and parasympatholytic properties of substituted phenols. 1. Heteroarylamine derivatives, *J. Med. Chem*. **26**, 808-813 (1983).

25. D.J.Holder, D.Allan, E.J.Land and S.Navaratnam, Establishment of pulse radiolysis facility on the SRS linac at Daresbury laboratory, in: *Proceedings of the 8th European particle accelerator conference*. Paris, France, pp. 2804-2806, European Physical Society (2002).

26. P.Wardman, Reduction potentials of one-electron couples involving free radicals in aqueous solution, *J. Phys. Chem. Ref. Data* **18**, 1637–1755 (1989).

27. A.Harriman, Further comments on the redox potentials of tryptophan and tyrosine. *J. Phys. Chem.* **91**, 6102–6104 (1987).

28. S.Foley, S.Navaratnam, D.J.McGarvey, E.J.Land, T.G.Truscott and C.A.Rice-Evans, Singlet oxygen quenching and the redox properties of hydroxycinnamic acids, *Free Radic. Biol. Med.* **26**, 1202-1208 (1999)

29. Gaussian 03, Revision C.02, M.J.Frisch, G.W.Trucks, H.B.Schlegel, G.E.Scuseria, M.A.Robb, J.R.Cheeseman, J.A.Montgomery, Jr., T.Vreven, K.N.Kudin, J.C.Burant, J.M.Millam, S.S.Iyengar, J.Tomasi, V.Barone, B.Mennucci, M.Cossi, G.Scalmani, N.Rega, G.A.Petersson, H.Nakatsuji, M.Hada, M.Ehara, K.Toyota, R.Fukuda, J.Hasegawa, M.Ishida, T.Nakajima, Y.Honda, O.Kitao, H.Nakai, M.Klene, X.Li, J.E.Knox, H.P.Hratchian, J.B.Cross, V.Bakken, C.Adamo, J.Jaramillo, R.Gomperts, R.E.Stratmann, O.Yazyev, A.J.Austin, R.Cammi, C.Pomelli, J.W.Ochterski, P.Y.Ayala, K.Morokuma, G.A.Voth, P.Salvador, J.J.Dannenberg, V.G.Zakrzewski, S.Dapprich, A.D.Daniels, M.C.Strain, O.Farkas, D.K.Malick, A.D.Rabuck, K.Raghavachari, J.B.Foresman, J.V.Ortiz, Q.Cui, A.G.Baboul, S.Clifford, J.Cioslowski, B.B.Stefanov, G.Liu, A.Liashenko, P.Piskorz, I.Komaromi, R.L.Martin, D.J.Fox, T.Keith, M.A.Al-Laham, C.Y.Peng, A.Nanayakkara, M.Challacombe, P.M.W.Gill, B.Johnson, W.Chen, M.W.Wong, C.Gonzalez and J.A.Pople, Gaussian, Inc., Wallingford CT, 2004.

30. A.Pezzella, O.Crescenzi, A.Natangelo, L.Panzella, A.Napolitano, S.Navaratnam, R.Edge, E.J.Land, V.Barone and M.d'Ischia, Chemical, pulse radiolysis and density functional studies of a new, labile 5,6-indolequinone and its semiquinone, *J. Org. Chem.* **72**, 1595 – 1603 (2007).

31. V.Male, Computational Studies of Anti-Malarials, M.Sc. Thesis, Department of Chemistry, University of Reading (2003).

32. Cambridge Crystallographic DataCentre, August 2008 update, www.ccdc.cam.ac.uk

33. S.M.Carter, A.Sia, M.J.Shaw and A.F. Heyduk, Isolation and characterization of a neutral imino-semiquinone radical, *J. Am. Chem. Soc.* **130**, 5838–5839 (2008).

34. D.Monti, B.Vodopivec, N.Basilico, P.Olliaro and D.Taramelli, A novel endogenous antimalarial: Fe(II)-Protoporphyrin IXR (Heme) inhibits hematin polymerization to β-hematin (malaria pigment) and kills malaria parasites, *Biochemistry* **38**, 8858-8863 (1999).

Table 1 – Second order rate constants (units, $dm^3\ mol^{-1}\ s^{-1}$) for reaction at neutral pH (unless otherwise indicated) of some inorganic radicals with pyronaridine and related compounds. [1]From reference [23]. [2]From reference [22].

Radical species	Pyronaridine	Amodiaquine[1]	APAP[2]	SA48
$N_3^{\bullet}$	3.5×10^9 (pH 6.8) 5.2×10^9 (pH 9.2)	1.2×10^9	3.8×10^9 (pH 7.1) 5.8×10^9 (pH 11.1)	2.4×10^9 (pH 6.8) 3.2×10^9 (pH 12.8)
$Br_2^{-\bullet}$	3.0×10^9 (pH 6.8)	2.1×10^8	2.5×10^7	----
$CCl_3O_2^{\bullet}$	1.8×10^9 (pH 7.7)	----	----	----

Table 2 - Dimensions in **1**, **2a**, **2b** and **3a**, distances, Å; torsion angles, °.

	1	**2a**	**2b**	**3a**
C2-N1	1.375	1.388	1.401	1.385
N1-C3	1.432	1.393	1.343	1.296
C1-C2-N1-C3	145.3	135.5	63.4	62.5
C2-N1-C3-C4	139.4	172.2	-170.9	-173.6
O7…N5	2.718	3.361	2.686	3.338

FIGURE LEGENDS

FIGURE 1 Structures of the antimalarial drugs pyronaridine (malaridine; Drug 7351 or 4-[(7-chloro-2-methoxybenzo[b]-1,5-naphthyridin-10-yl)amino]-2,6-bis(1-pyrrolidinylmethyl)- phenol) and amodiaquine (4-(7-chloroquinolin-4-ylamino)-2-((diethylamino)methyl)phenol), together with that of the model compound SA48 (*N*-(4-hydroxy-3,5-bis(pyrrolidin-1-ylmethyl)phenyl)acetamide). The table indicates the pK_a values and sites of ionization in the pyronaridine molecule (from reference [11]).

FIGURE 2 A: Transient spectra formed by oxidation of pyronaridine by azidyl radical in N_2O-saturated solutions containing pyronaridine (50 μmol dm^{-3}) and sodium azide (0.1 mol dm^{-3}) at pH 5.4 40 μs after the pulse (●), pH 6.7 40 μs after the pulse (○), pH 7.6 20 μs after the pulse (■) and pH 8.8 20 μs after the pulse (▲). B:- Transient spectra from oxidation of pyronaridine (50 μmol dm^{-3}) by $Br_2^{-\bullet}$ in N_2O-saturated solution containing KBr (0.1 mol dm^{-3}) at pH 6.8 40 μs after the pulse (□), and by trichloromethylperoxyl radical at pH 7.7 50 μs after the pulse (♦) in a solution saturated with N_2O/O_2 (4:1 v/v) and containing propan-2-ol (3.3 mol dm^{-3}), acetone (1.4 mol dm^{-3}) and carbon tetrachloride (12 mmol dm^{-3}). Dose = 9 Gy per pulse. The absorption spectrum of unirradiated pyronaridine (50 μmol dm^{-3}) at pH 8.8 is shown for comparison (solid line).

FIGURE 3 Transient absorption spectra form one-electron oxidation of SA48 by azidyl radicals at pH 6.8 (♦) and at pH 12.8 (□).

FIGURE 4 Oxidation pyronaridine by tryptophan radicals demonstrated by formation of the pyronaridine radical transient absorption at 640 nm in N_2O-saturated solutions at pH 7 containing NaN_3 (0.1 mol dm^{-3}) and tryptophan (2.5 mmol dm^{-3}) (a); and together with pyronaridine at concentrations of 50 (b); 100 (c); 150 (d) and 200 (e) μmol dm^{-3}. INSET: effect of tryptophan concentration on the first order rate for formation of the transient absorbance at 640 nm fir the above solutions.

FIGURE 5 The transient absorption change in an N_2O-saturated solution at pH 7 containing APAP (4 mmol dm^{-3}) and pyronaridine (1 mmol dm^{-3}) recorded at 640 nm.

FIGURE 6 Reduction of the pyronaridine radical recorded at 640 nm by pulse radiolysis of N_2O-saturated solutions of pyronaridine (1 mmol dm^{-3}) and NaN_3 (0.1 mol dm^{-3}) at pH 6.8 alone and with increasing concentrations of ascorbate (90, 180, 300 and 500 μmol dm^{-3}). INSET:- Second order plots for the reduction of pyronaridine radical absorption at 640 nm and pH 6.8 by ascorbate (■) and caffeic acid (□).

FIGURE 7 Decay of the transient difference spectra on a millisecond timescale following pulse radiolysis of an N_2O-saturated solution of pyronaridine

(50 μmol dm^{-3}) containing sodium azide (0.1 mol dm^{-3}) and phosphate buffer (20 mmol dm^{-3}) at pH 6.7. Spectra are shown at delays after the pulse of 50 μs (■), 200 μs (□), 500 μs (♦), 1.5 ms (○) and 8 ms (∗). Inset: decay of the transient absorption at 640 nm.

FIGURE 8 Disproportionation of Pyronaridine radicals. **1:** pyronaridine); **2a**: phenoxyl radical; **2b**: aminyl radical; **3a** Pyronaridine quinone: 4-(7-chloro-2-methoxybenzo[*b*][1,5]naphthyridin-10-ylimino)-2,6-bis(pyrrolidin-1-ylmethyl)cyclohexa-2,5-dienone.

FIGURE 9 Structure of pyronaridine **1,** the two radicals **2a** and **2b,** and the iminoquinone **3a**.

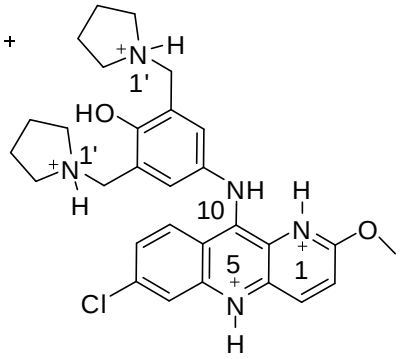

Pyronaridine

pK_a value	Assignment
7.08	N_1 of naphthyridine
7.39	N_5 of naphthyridine
9.88	N of pyrrolidine
10.25	-NH or –OH of aminophenol

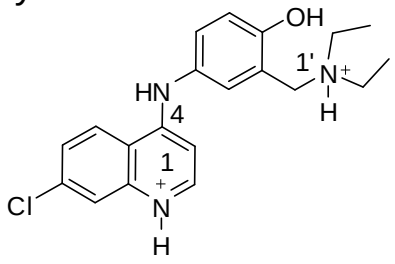

Amodiaquine

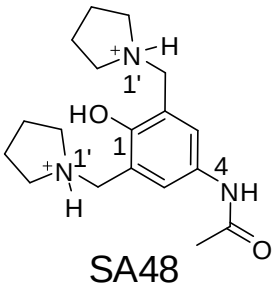

SA48

FIGURE 1

FIGURE 2

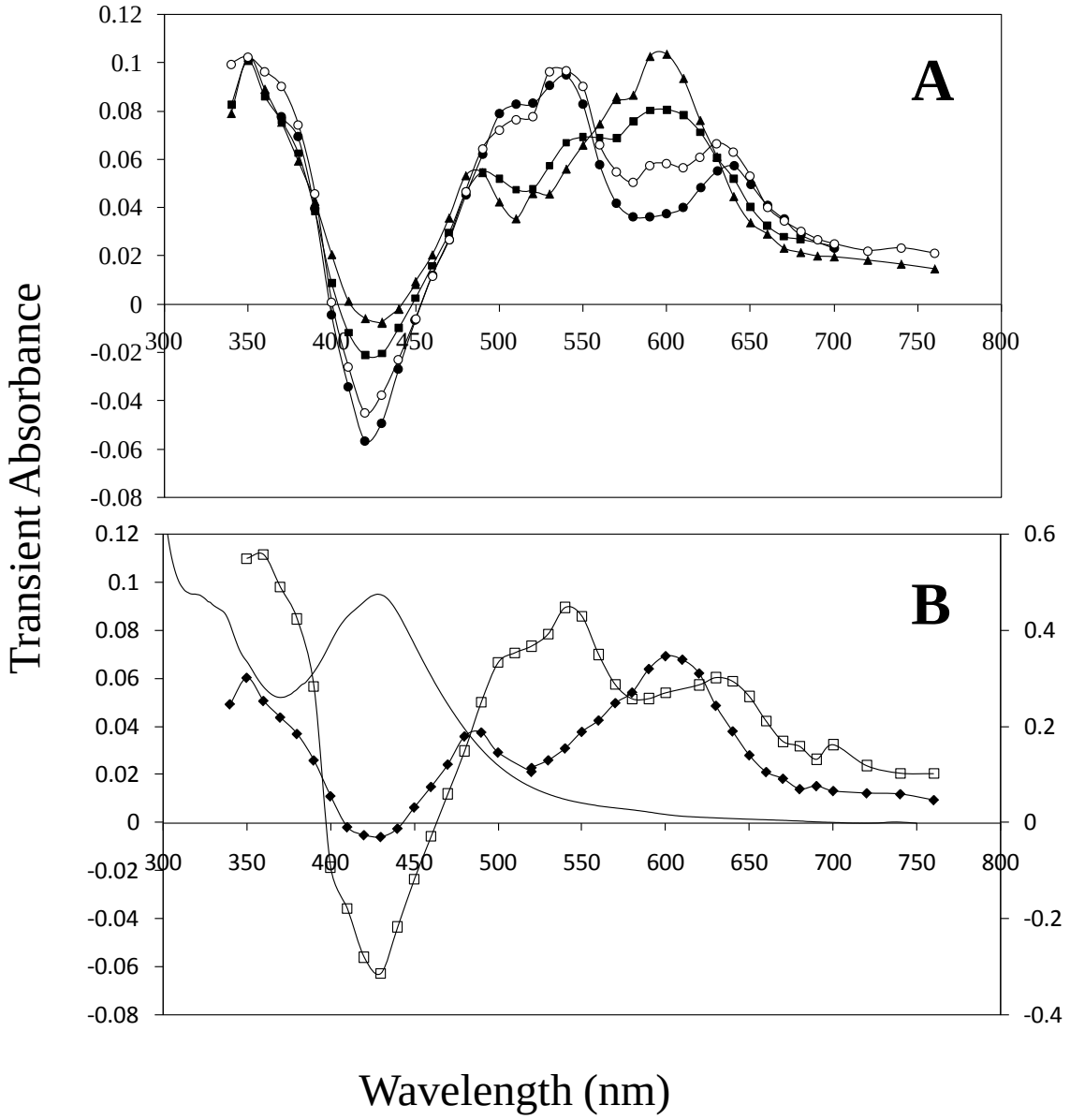
A
B
Transient Absorbance
Wavelength (nm)
0.12
0.1
0.08
0.06
0.04
0.02
0
-0.02
-0.04
-0.06
-0.08
0.6
0.4
0.2
-0.2
-0.4
300
350
400
450
500
550
600
650
700
750
800

FIGURE 3

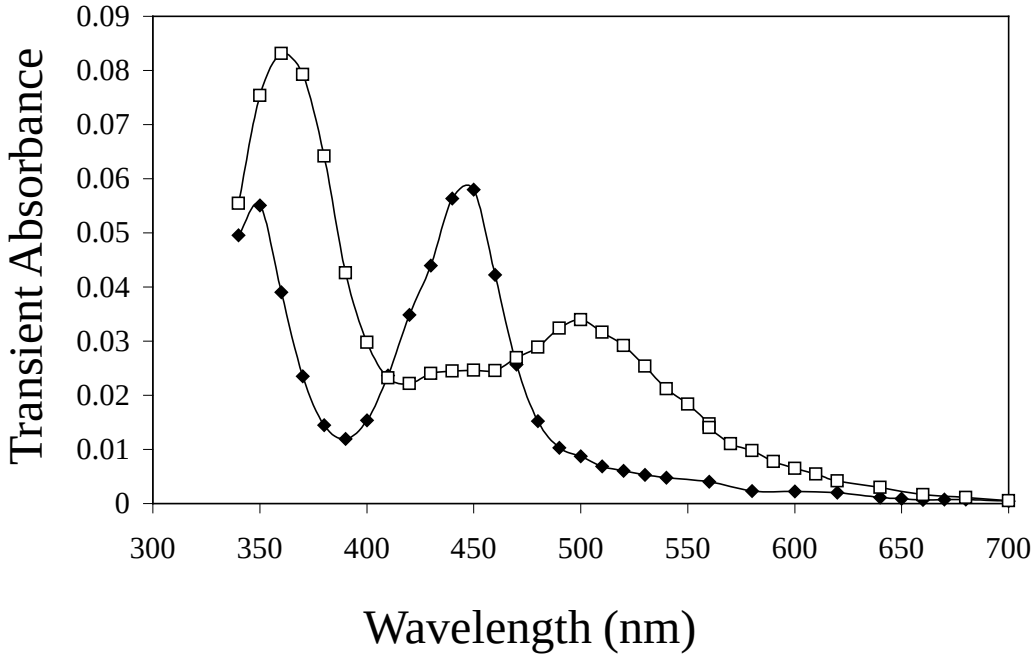
Transient Absorbance
0.09
0.08
0.07
0.06
0.05
0.04
0.03
0.02
0.01
0
300
350
400
450
500
550
600
650
700
Wavelength (nm)

FIGURE 4

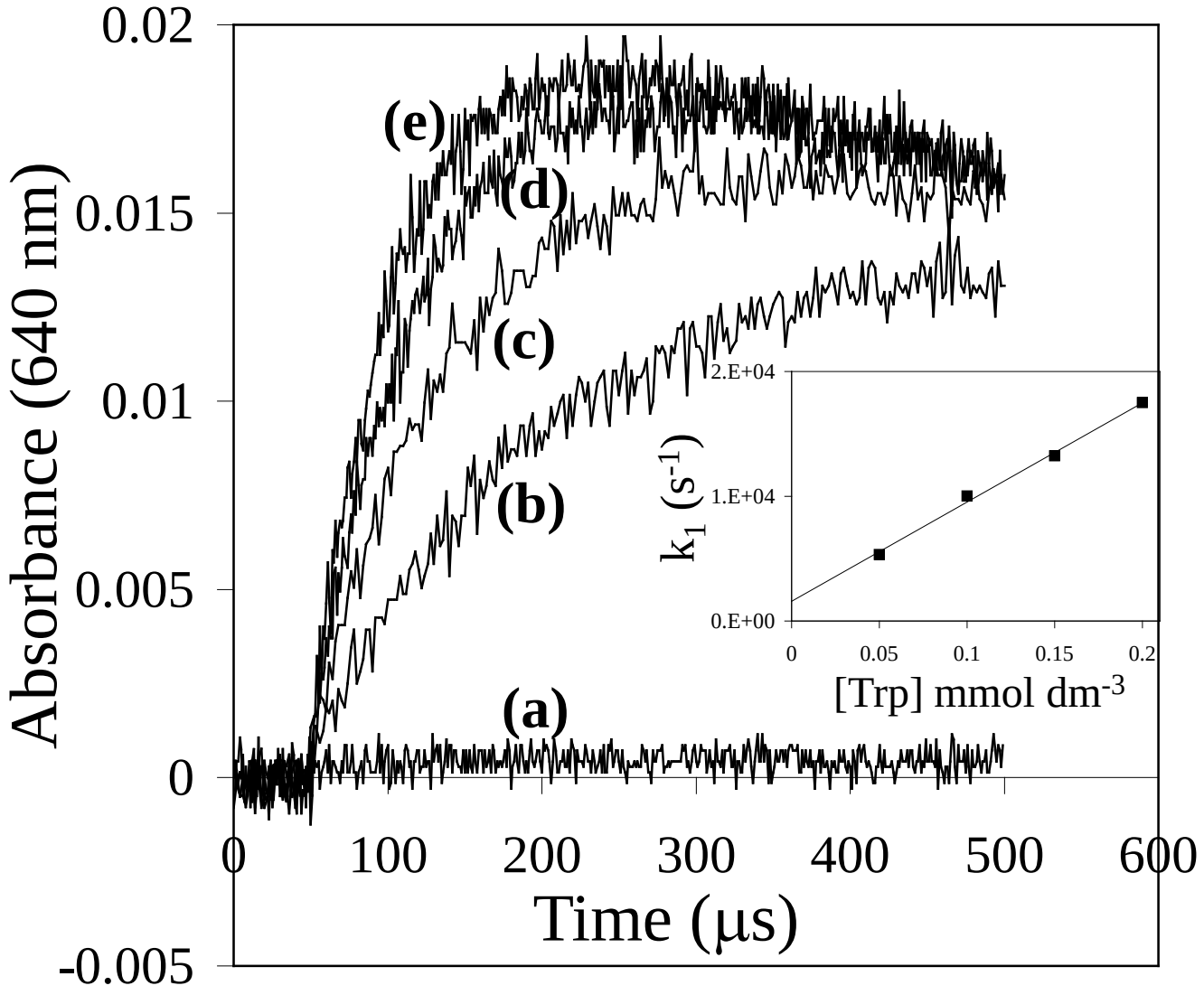
0.02
0.015
0.01
0.005
0
-0.005
Absorbance (640 nm)
0
100
200
300
400
500
600
Time (μs)
(e)
(d)
(c)
(b)
(a)
2.E+04
1.E+04
0.E+00
k1 (s-1)
0
0.05
0.1
0.15
0.2
[Trp] mmol dm-3

FIGURE 5

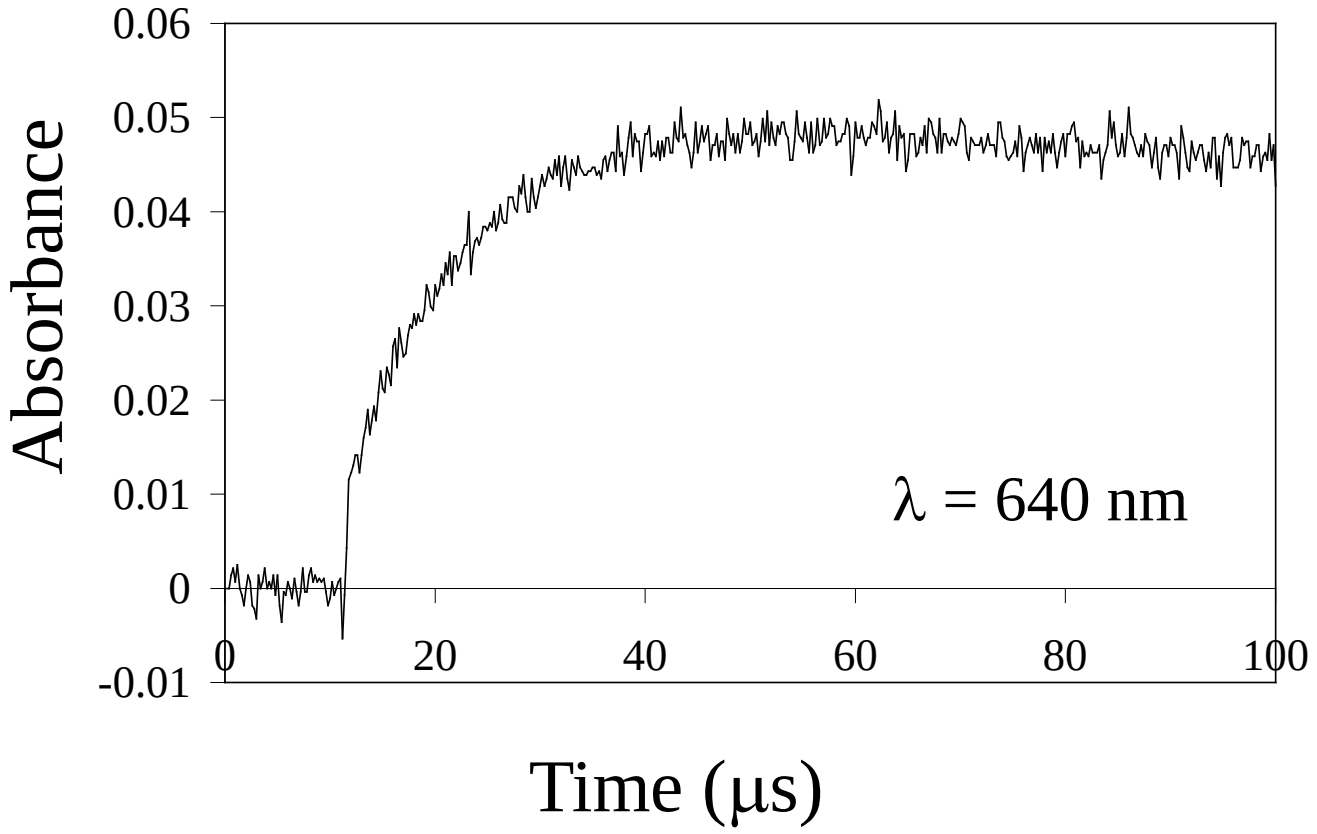
0.06
0.05
0.04
0.03
0.02
0.01
0
-0.01
Absorbance
0
20
40
60
80
100
λ = 640 nm
Time (μs)

FIGURE 6

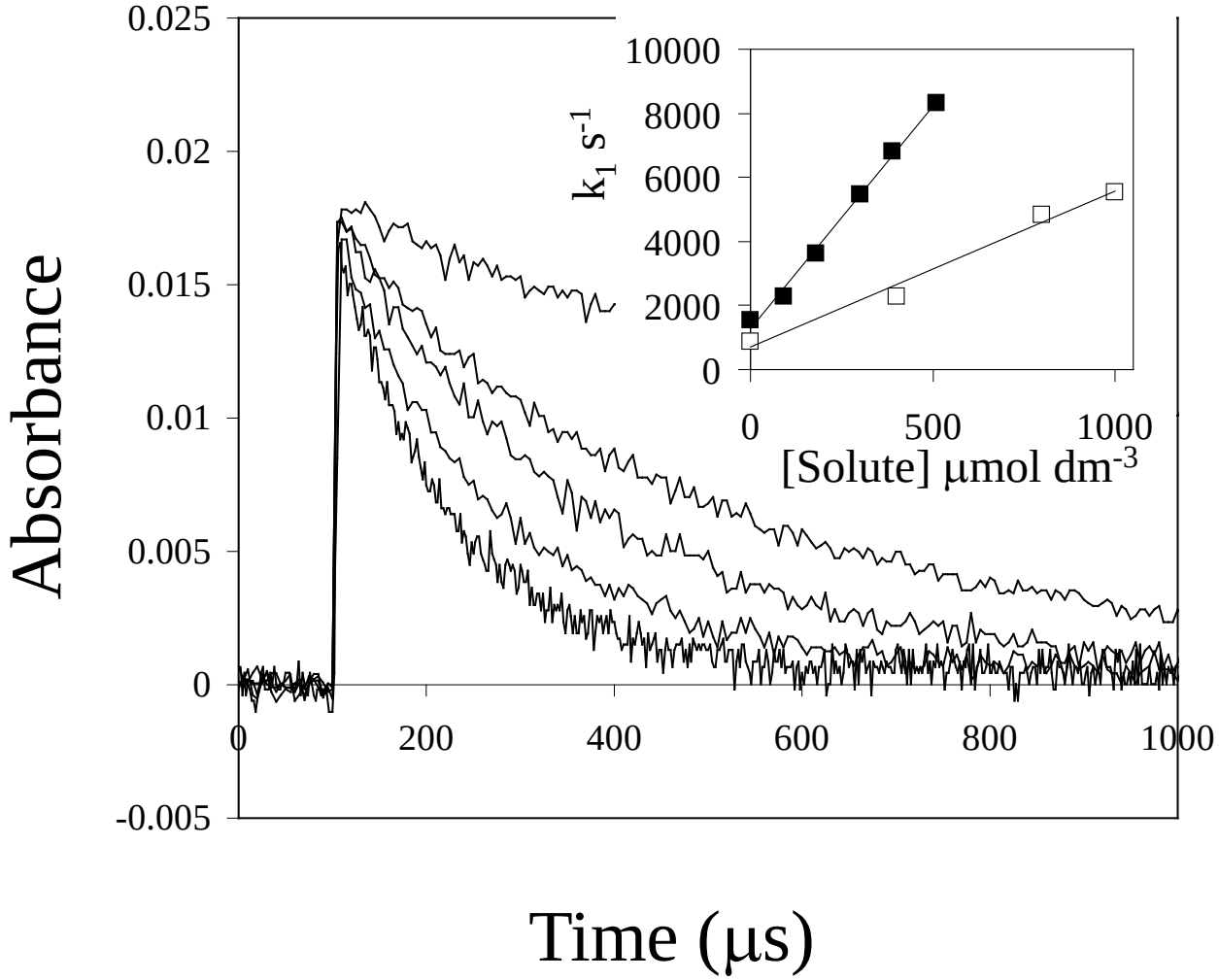
0.025
0.02
0.015
0.01
0.005
0
-0.005
Absorbance
0
200
400
600
800
1000
Time (μs)
10000
8000
6000
4000
2000
0
k_1 s^{-1}
0
500
1000
[Solute] μmol dm^{-3}

FIGURE 7

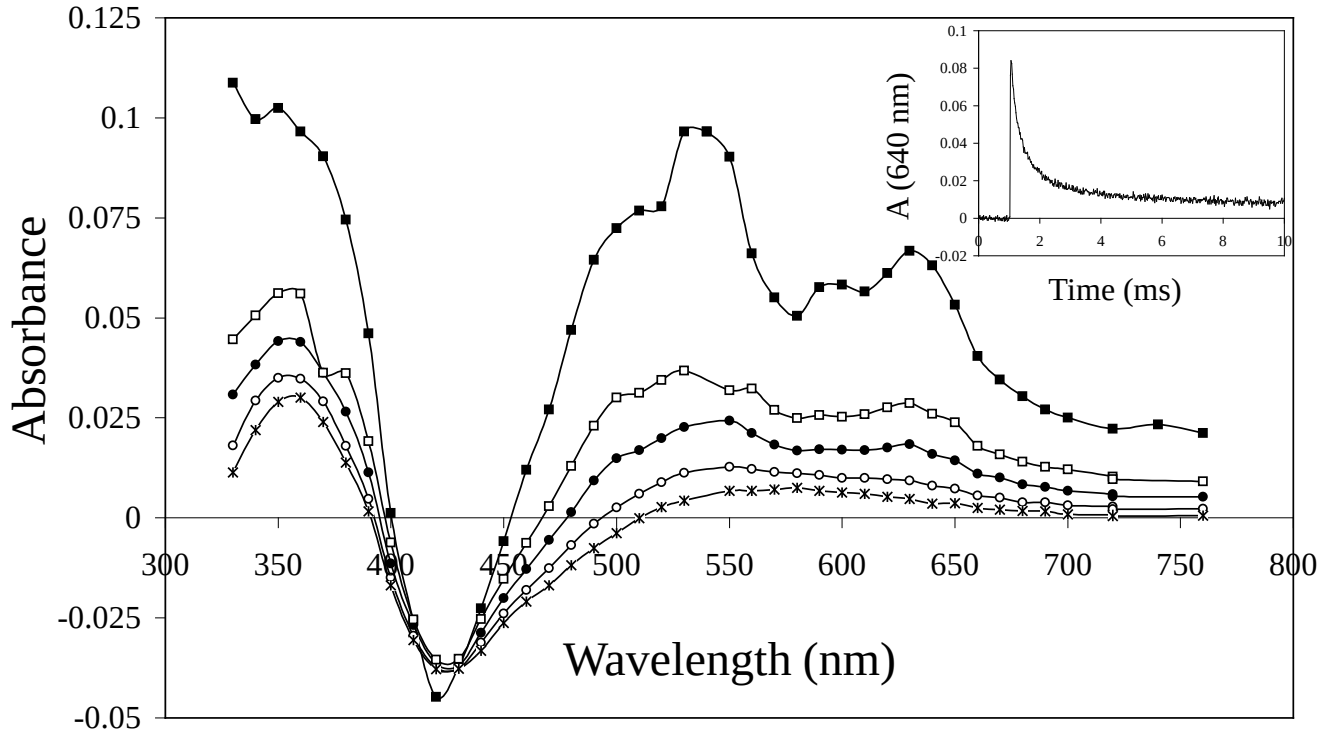
0.125
0.1
0.075
0.05
0.025
0
-0.025
-0.05
Absorbance
300
350
400
450
500
550
600
650
700
750
800
Wavelength (nm)
A (640 nm)
0.1
0.08
0.06
0.04
0.02
0
-0.02
0
2
4
6
8
10
Time (ms)

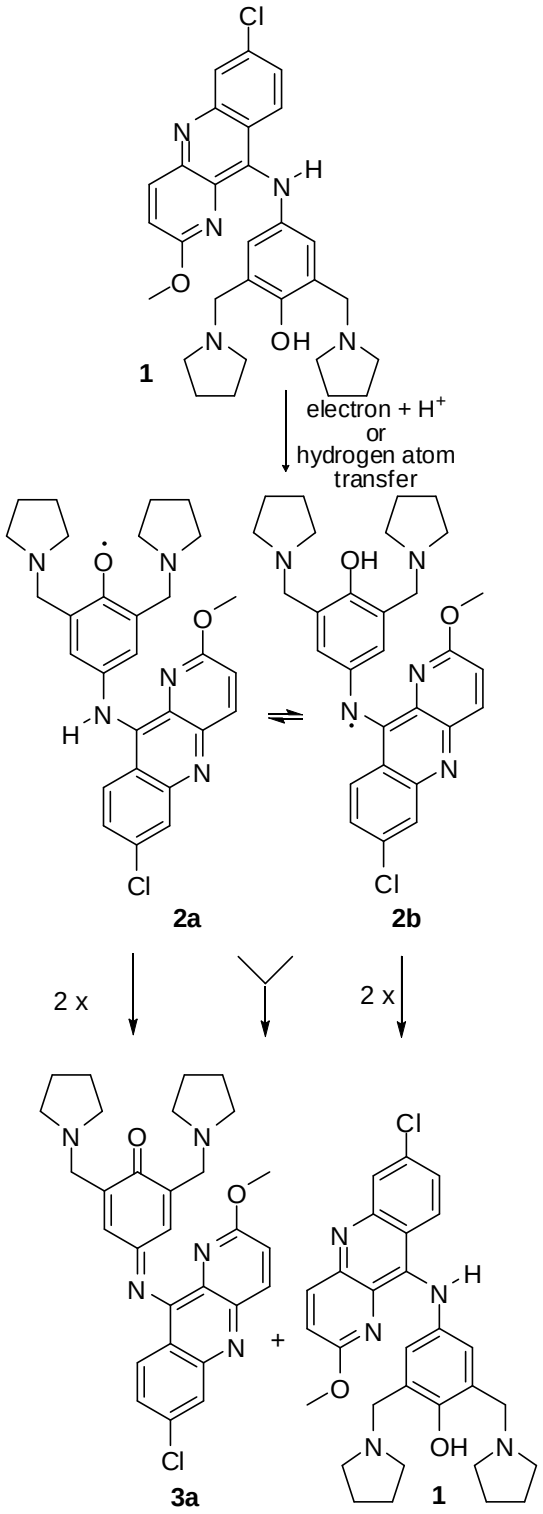
Cl
N
H
N
N
O
N
OH
N
1
electron + H+
or
hydrogen atom
transfer
N
O
N
N
OH
N
O
O
N
N
H
N
N
N
N
Cl
Cl
2a
2b
2 x
2 x
N
O
N
O
N
N
N
N
Cl
+
Cl
N
H
N
N
O
N
OH
N
3a
1

FIGURE 8

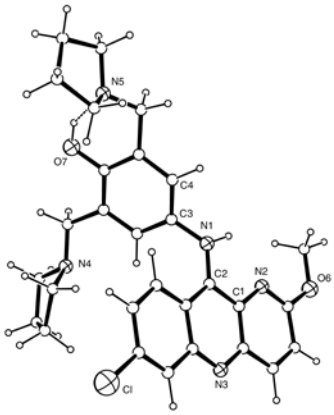

1

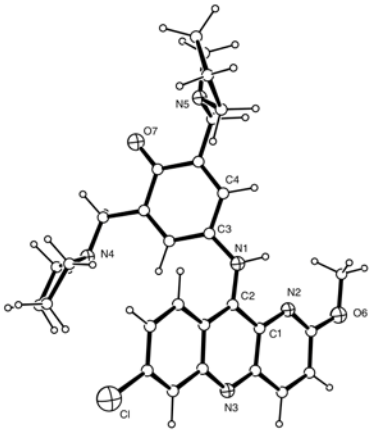

2a

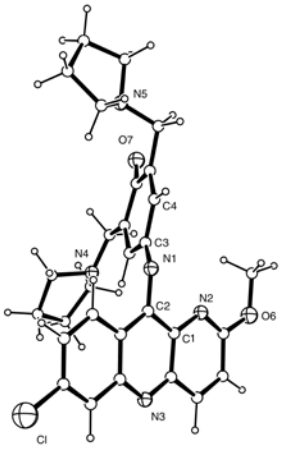

3a

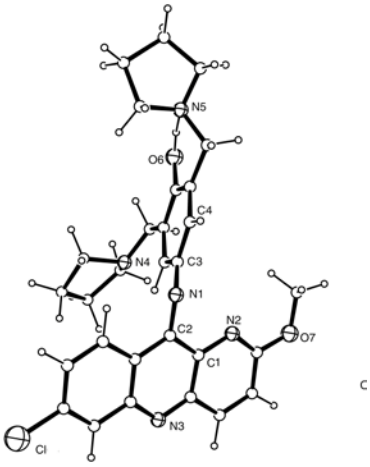

2b

FIGURE 9

A PULSE RADIOLYSIS STUDY OF FREE RADICALS FORMED BY ONE ELECTRON OXIDATION OF THE ANTIMALARIAL DRUG PYRONARIDINE.

F.M.D.Ismail, M.G.B.Drew, S.Navaratnam and R.H.Bisby

SUPPLEMENTARY MATERIAL

A – RESULTS FROM DFT CALCULATIONS

B – DATA FROM ELECTROSPRAY MASS SPECTROMETRY

A -- RESULTS FROM DFT CALCULATIONS

1: pyronaridine [malaridine, Drug 7351 or Pyronaridine (4-[(7-chloro-2-methoxybenzo[b]-1,5-naphthyridin-10-yl)amino]-2,6-bis(1-pyrrolidinylmethyl)-phenol); **2a**: phenoxyl radical; **2b**: aminyl radical; **3a** Pyronaridine quinone: 4-(6-chloro-2-methoxyacridin-9-ylimino)-2,6-bis(pyrrolidin-1-ylmethyl)cyclohexa-2,5-dienone.

==========

STRUCTURE OF 1

SCF Done: E(RB+HF-LYP) = -2008.82200761 A.U. after 19 cycles

Standard orientation:

Center Number	Atomic Number	Atomic Type	Coordinates (Angstroms) X	Y	Z
1	6	0	-1.509253	-1.872551	-0.558419
2	6	0	-0.387286	-1.283390	0.029153
3	7	0	0.914835	-1.648679	-0.444302

4	6	0	1.988642	-0.814107	-0.645392
5	6	0	3.280059	-1.347494	-0.377022
6	6	0	4.427375	-0.525192	-0.585063
7	7	0	4.378412	0.740434	-1.026829
8	6	0	3.162077	1.237601	-1.324834
9	6	0	1.924364	0.506009	-1.178837
10	6	0	0.719081	1.124493	-1.628784
11	6	0	0.711273	2.395977	-2.149540
12	6	0	1.929630	3.120193	-2.236021
13	17	0	1.884503	4.755687	-2.885470
14	6	0	3.119777	2.570448	-1.843117
15	1	0	4.057160	3.109081	-1.927109
16	1	0	-0.210974	2.849030	-2.498270
17	1	0	-0.213989	0.577550	-1.574192
18	6	0	5.701490	-1.113762	-0.284407
19	6	0	5.773835	-2.398709	0.166932
20	6	0	4.551169	-3.128729	0.335374
21	8	0	4.697204	-4.395912	0.787900
22	6	0	3.510022	-5.171168	0.981271
23	1	0	2.967218	-5.290155	0.037868
24	1	0	3.856499	-6.139216	1.346074
25	1	0	2.853090	-4.697314	1.717727
26	7	0	3.366223	-2.639167	0.085831
27	1	0	6.714506	-2.884784	0.404085
28	1	0	6.588938	-0.505479	-0.433022

29	1	0	1.229308	-2.571169	-0.151057
30	6	0	-0.557493	-0.399200	1.101605
31	6	0	-1.829722	-0.071387	1.572002
32	1	0	-4.850872	-0.681295	0.789554
33	6	0	-2.036363	0.867935	2.747469
34	7	0	-0.879055	1.697720	3.051599
35	6	0	-0.677640	2.835314	2.146325
36	6	0	0.382474	3.694993	2.861697
37	6	0	0.233787	3.319205	4.365832
38	6	0	-0.917350	2.297475	4.388387
39	1	0	-0.802536	1.525980	5.158366
40	1	0	-1.884573	2.811524	4.567973
41	1	0	1.155937	2.863912	4.741640
42	1	0	0.014402	4.186351	4.997518
43	1	0	1.386168	3.451529	2.499101
44	1	0	0.219525	4.761947	2.677598
45	1	0	-0.364990	2.499405	1.153143
46	1	0	-1.621817	3.406223	2.024751
47	1	0	-2.261844	0.264536	3.638035
48	1	0	-2.939148	1.481108	2.566324
49	1	0	0.304628	0.050717	1.584420
50	1	0	-1.373365	-2.555535	-1.394331
51	8	0	-4.186924	-0.370001	1.463737
52	6	0	-2.950788	-0.680004	0.973908
53	6	0	-2.796006	-1.598760	-0.084358

54	6	0	-3.998528	-2.331456	-0.647400
55	7	0	-5.171013	-1.463386	-0.822781
56	6	0	-5.058673	-0.480585	-1.914438
57	6	0	-6.491607	0.060770	-2.066830
58	6	0	-7.402070	-1.090764	-1.544789
59	6	0	-6.418435	-2.191709	-1.104712
60	1	0	-6.745240	-2.744898	-0.217730
61	1	0	-6.260661	-2.922802	-1.920245
62	1	0	-8.005743	-0.751735	-0.696820
63	1	0	-8.092900	-1.458577	-2.309900
64	1	0	-6.625897	0.962828	-1.461439
65	1	0	-6.707634	0.329520	-3.105528
66	1	0	-4.322192	0.289287	-1.666530
67	1	0	-4.725753	-0.981112	-2.843387
68	1	0	-3.727393	-2.827286	-1.597338
69	1	0	-4.297482	-3.125679	0.052042

STRUCTURE OF 3a

SCF Done: E(RB+HF-LYP) = -2007.57446479 A.U. after 18 cycles

Standard orientation:

Center Number	Atomic Number	Atomic Type	Coordinates (Angstroms) X	Y	Z

1	6	0	-2.004275	0.756707	-1.351592

2	6	0	-0.704737	0.305475	-0.843573
3	7	0	0.344849	0.900972	-1.317432
4	6	0	1.650443	0.523787	-1.051105
5	6	0	2.165471	-0.741911	-1.428215
6	6	0	3.568822	-0.982523	-1.221603
7	7	0	4.420109	-0.099137	-0.687605
8	6	0	3.932531	1.110980	-0.347591
9	6	0	2.555505	1.485855	-0.527869
10	6	0	2.145214	2.799104	-0.157125
11	6	0	3.038953	3.698044	0.372315
12	6	0	4.393277	3.308438	0.561270
13	17	0	5.506629	4.480690	1.252109
14	6	0	4.839813	2.059848	0.215752
15	1	0	5.873075	1.760499	0.352375
16	1	0	2.727312	4.700959	0.644889
17	1	0	1.109784	3.085366	-0.311151
18	6	0	4.068691	-2.271818	-1.612480
19	6	0	3.229069	-3.189956	-2.165014
20	6	0	1.849210	-2.827189	-2.339967
21	8	0	1.081569	-3.778939	-2.912444
22	6	0	-0.301247	-3.469465	-3.134945
23	1	0	-0.399966	-2.599602	-3.791172
24	1	0	-0.719075	-4.358960	-3.608243
25	1	0	-0.807001	-3.263018	-2.187295
26	7	0	1.336787	-1.678983	-1.992203

27	1	0	3.560326	-4.173103	-2.482870
28	1	0	5.124510	-2.473216	-1.457466
29	6	0	-0.693117	-0.726684	0.195588
30	6	0	-1.834567	-1.288714	0.646918
31	6	0	-1.867575	-2.364317	1.710536
32	7	0	-0.616082	-2.508966	2.436463
33	6	0	-0.398934	-1.518566	3.499361
34	6	0	0.800158	-2.077699	4.289868
35	6	0	0.776135	-3.607644	3.999976
36	6	0	-0.460403	-3.805361	3.105713
37	1	0	-0.341319	-4.605568	2.366663
38	1	0	-1.349180	-4.045585	3.724082
39	1	0	1.683351	-3.911995	3.468135
40	1	0	0.712675	-4.208379	4.913039
41	1	0	1.737353	-1.632171	3.941137
42	1	0	0.710180	-1.852283	5.357450
43	1	0	-0.216132	-0.523733	3.080518
44	1	0	-1.293469	-1.445572	4.150837
45	1	0	-2.098244	-3.317626	1.215569
46	1	0	-2.722153	-2.174520	2.386647
47	1	0	0.258758	-1.037241	0.613435
48	1	0	-1.976212	1.552111	-2.092979
49	8	0	-4.168205	-1.529925	0.331948
50	6	0	-3.145826	-0.909578	0.042702
51	6	0	-3.169478	0.211313	-0.943979

52	6	0	-4.518447	0.672822	-1.441030
53	7	0	-5.171478	1.548899	-0.474772
54	6	0	-4.666606	2.921932	-0.427164
55	6	0	-5.704559	3.665358	0.436709
56	6	0	-7.008690	2.826577	0.285736
57	6	0	-6.617940	1.682136	-0.666958
58	1	0	-7.119468	0.734819	-0.442506
59	1	0	-6.857661	1.954661	-1.716095
60	1	0	-7.321431	2.425265	1.254901
61	1	0	-7.842590	3.413893	-0.112384
62	1	0	-5.383895	3.694511	1.483011
63	1	0	-5.830277	4.700889	0.103886
64	1	0	-3.654526	2.954868	-0.010833
65	1	0	-4.624607	3.362350	-1.446270
66	1	0	-4.404528	1.166802	-2.426734
67	1	0	-5.155813	-0.206426	-1.577022

STRUCTURE OF 2a

SCF Done: E(UB+HF-LYP) = -2008.18201945 A.U. after 33 cycles

Standard orientation:

Center Number	Atomic Number	Atomic Type	Coordinates (Angstroms) X	Y	Z

1	6	0	-2.039188	1.479846	-0.038479
2	6	0	-0.765675	0.872080	-0.209479
3	7	0	0.333363	1.559932	0.299203
4	6	0	1.659961	1.167283	0.416881
5	6	0	2.642688	2.111483	0.032456
6	6	0	4.020757	1.740717	0.128985
7	7	0	4.446841	0.553607	0.580251
8	6	0	3.515470	-0.315939	1.018607
9	6	0	2.094813	-0.056772	0.989121
10	6	0	1.221891	-1.001424	1.605336
11	6	0	1.702966	-2.158036	2.167405
12	6	0	3.096946	-2.433530	2.123320
13	17	0	3.671327	-3.938291	2.823521
14	6	0	3.983966	-1.547851	1.572599
15	1	0	5.052038	-1.734530	1.561351
16	1	0	1.032235	-2.861092	2.650292
17	1	0	0.158391	-0.795683	1.649794
18	6	0	4.981582	2.716007	-0.302496
19	6	0	4.562099	3.931096	-0.755378
20	6	0	3.151226	4.196367	-0.790592
21	8	0	2.814103	5.421942	-1.240428
22	6	0	1.420531	5.748925	-1.313434
23	1	0	0.963987	5.712951	-0.319258
24	1	0	1.386426	6.763759	-1.711327
25	1	0	0.896335	5.056891	-1.979400

26	7	0	2.232515	3.339719	-0.425972
27	1	0	5.249004	4.702312	-1.087699
28	1	0	6.033786	2.453324	-0.247218
29	1	0	0.254093	2.572164	0.236418
30	6	0	-0.658849	-0.343470	-0.931757
31	6	0	-1.771485	-0.930056	-1.489833
32	6	0	-1.691732	-2.161284	-2.365889
33	7	0	-0.452725	-2.915744	-2.234482
34	6	0	-0.400668	-3.806150	-1.068290
35	6	0	0.828169	-4.696883	-1.333202
36	6	0	0.995178	-4.671513	-2.881458
37	6	0	-0.169203	-3.794073	-3.374823
38	1	0	0.076585	-3.200830	-4.262793
39	1	0	-1.048638	-4.423173	-3.622065
40	1	0	1.955293	-4.223027	-3.156986
41	1	0	0.960497	-5.671973	-3.325005
42	1	0	1.716398	-4.288163	-0.841077
43	1	0	0.677049	-5.709218	-0.944156
44	1	0	-0.326819	-3.231926	-0.139733
45	1	0	-1.321162	-4.422484	-1.008665
46	1	0	-1.785909	-1.829875	-3.409699
47	1	0	-2.581596	-2.790728	-2.181676
48	1	0	0.310464	-0.800412	-1.102849
49	1	0	-2.103713	2.398445	0.544251
50	8	0	-4.093568	-0.772588	-1.956631

51	6	0	-3.091739	-0.299322	-1.363779
52	6	0	-3.181289	0.922367	-0.558017
53	6	0	-4.545730	1.533738	-0.350549
54	7	0	-5.295008	0.876826	0.714026
55	6	0	-4.827865	1.141906	2.074884
56	6	0	-5.950722	0.572505	2.963382
57	6	0	-7.221090	0.628174	2.063932
58	6	0	-6.718406	1.214738	0.731002
59	1	0	-7.219101	0.794430	-0.147892
60	1	0	-6.868629	2.315351	0.712426
61	1	0	-7.629293	-0.375800	1.910857
62	1	0	-8.015312	1.244362	2.498078
63	1	0	-5.725547	-0.460187	3.248503
64	1	0	-6.063074	1.151499	3.885998
65	1	0	-3.854832	0.674345	2.253967
66	1	0	-4.713289	2.233846	2.250322
67	1	0	-4.445712	2.623767	-0.156597
68	1	0	-5.119321	1.411813	-1.275464

STRUCTURE OF 2b

SCF Done: E(UB+HF-LYP) = -2008.18284432 A.U. after 27 cycles

Standard orientation:

Center	Atomic	Atomic	Coordinates (Angstroms)		
Number	Number	Type	X	Y	Z

1	6	0	1.820453	-0.267508	-1.696406
2	6	0	0.561344	-0.017170	-1.049686
3	7	0	-0.552109	-0.337772	-1.728757
4	6	0	-1.819944	0.038382	-1.265541
5	6	0	-2.232396	1.380753	-1.130600
6	6	0	-3.602600	1.630727	-0.770318
7	7	0	-4.515329	0.677750	-0.538516
8	6	0	-4.116453	-0.603612	-0.663619
9	6	0	-2.778089	-0.977036	-1.034834
10	6	0	-2.441687	-2.358211	-1.131892
11	6	0	-3.376587	-3.332398	-0.880428
12	6	0	-4.697851	-2.951232	-0.515185
13	17	0	-5.869977	-4.225856	-0.198002
14	6	0	-5.070031	-1.636262	-0.404487
15	1	0	-6.075733	-1.343831	-0.124332
16	1	0	-3.125031	-4.385133	-0.958681
17	1	0	-1.429465	-2.627258	-1.422458
18	6	0	-3.998623	3.006885	-0.660792
19	6	0	-3.096829	3.999245	-0.899311
20	6	0	-1.757106	3.625769	-1.261955
21	8	0	-0.925153	4.668088	-1.495880
22	6	0	0.418600	4.360602	-1.888845
23	1	0	0.425528	3.775637	-2.814095
24	1	0	0.898550	5.328426	-2.039842

25	1	0	0.929488	3.793258	-1.104833
26	7	0	-1.336600	2.397819	-1.374374
27	1	0	-3.349809	5.052700	-0.838753
28	1	0	-5.030236	3.214451	-0.392639
29	6	0	0.616294	0.455891	0.305824
30	6	0	1.809012	0.642767	0.974658
31	1	0	4.894431	0.077710	0.409137
32	6	0	1.841581	1.109879	2.420051
33	7	0	0.610985	0.809781	3.138442
34	6	0	0.454515	-0.598046	3.517793
35	6	0	-0.729622	-0.586740	4.505471
36	6	0	-0.753952	0.866523	5.065369
37	6	0	0.449179	1.550421	4.392209
38	1	0	0.287730	2.615675	4.190601
39	1	0	1.352028	1.458735	5.031327
40	1	0	-1.684142	1.370898	4.784781
41	1	0	-0.677595	0.899495	6.157169
42	1	0	-1.666437	-0.821116	3.989715
43	1	0	-0.594950	-1.335133	5.293329
44	1	0	0.276647	-1.224680	2.637208
45	1	0	1.374263	-0.973588	4.013309
46	1	0	1.987308	2.199269	2.434242
47	1	0	2.724609	0.679241	2.926904
48	1	0	-0.308990	0.631276	0.845381
49	1	0	1.787167	-0.621862	-2.724518

50	8	0	4.193879	0.557517	0.949974
51	6	0	3.026061	0.392233	0.287650
52	6	0	3.025659	-0.048771	-1.064840
53	6	0	4.341852	-0.199293	-1.804824
54	7	0	5.363771	-0.878427	-0.995774
55	6	0	5.125686	-2.324578	-0.822313
56	6	0	6.453884	-2.852471	-0.250286
57	6	0	7.524712	-1.837102	-0.749394
58	6	0	6.724543	-0.793032	-1.551797
59	1	0	7.111364	0.226811	-1.455246
60	1	0	6.715061	-1.050369	-2.627049
61	1	0	8.038550	-1.367427	0.095301
62	1	0	8.289365	-2.310371	-1.373409
63	1	0	6.420676	-2.872568	0.843788
64	1	0	6.655114	-3.873600	-0.587739
65	1	0	4.262302	-2.503786	-0.175198
66	1	0	4.912056	-2.786241	-1.803867
67	1	0	4.178132	-0.731011	-2.758801
68	1	0	4.737177	0.795350	-2.054651

B – DATA FROM ELECTROSPRAY MASS SPECTROMETRY

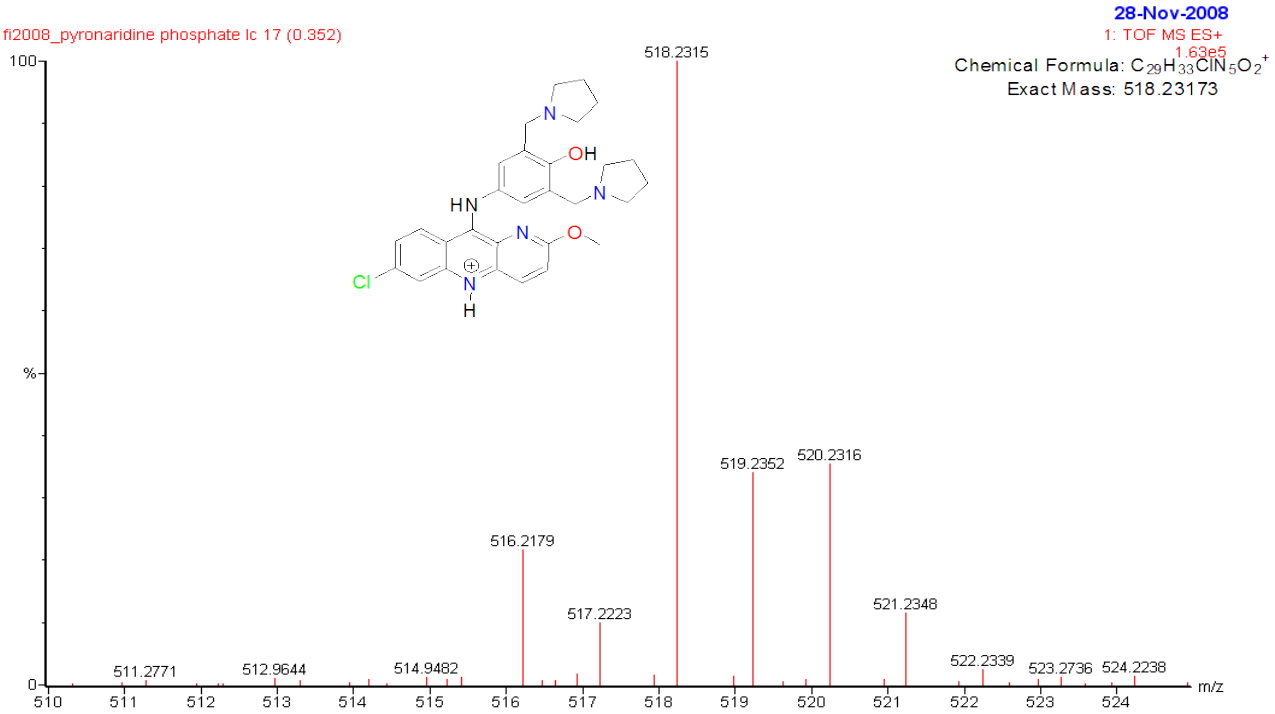

Supp Figure 1: Positive ion high resolution electrospray mass spectrum of authentic protonated Pyronaridine (7-chloro-10-(4-hydroxy-3,5-bis(pyrrolidin-1-ylmethyl)phenylamino)-2-methoxybenzo[b][1,5]naphthyridin-5-ium). Note presence of peak with reduced intensity ascribed to spontaneous formation of iminoquinone during electrospray conditions.

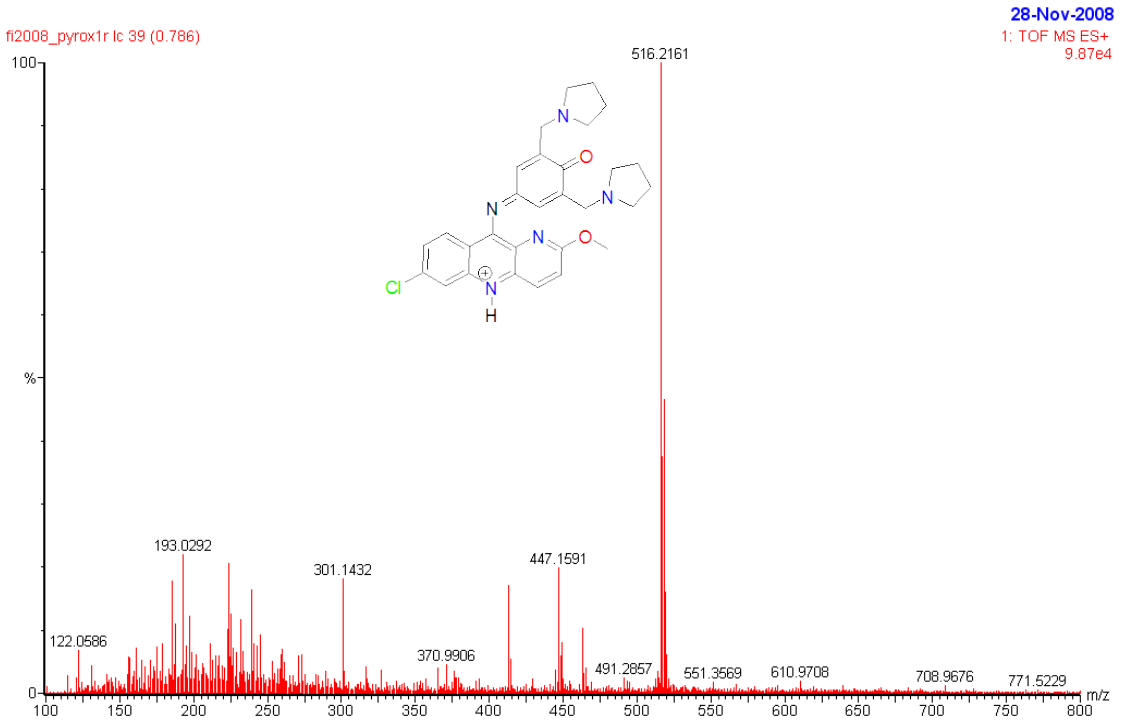

Supp Figure 2: Positive ion high resolution electrospray mass spectrum of authentic protonated iminoquinone (7-chloro-2-methoxy-10-(4-oxo-3,5-bis(pyrrolidin-1-ylmethyl)cyclohexa-2,5dienylideneamino) benzo[b] [1,5]naphth-yridin-5-ium)

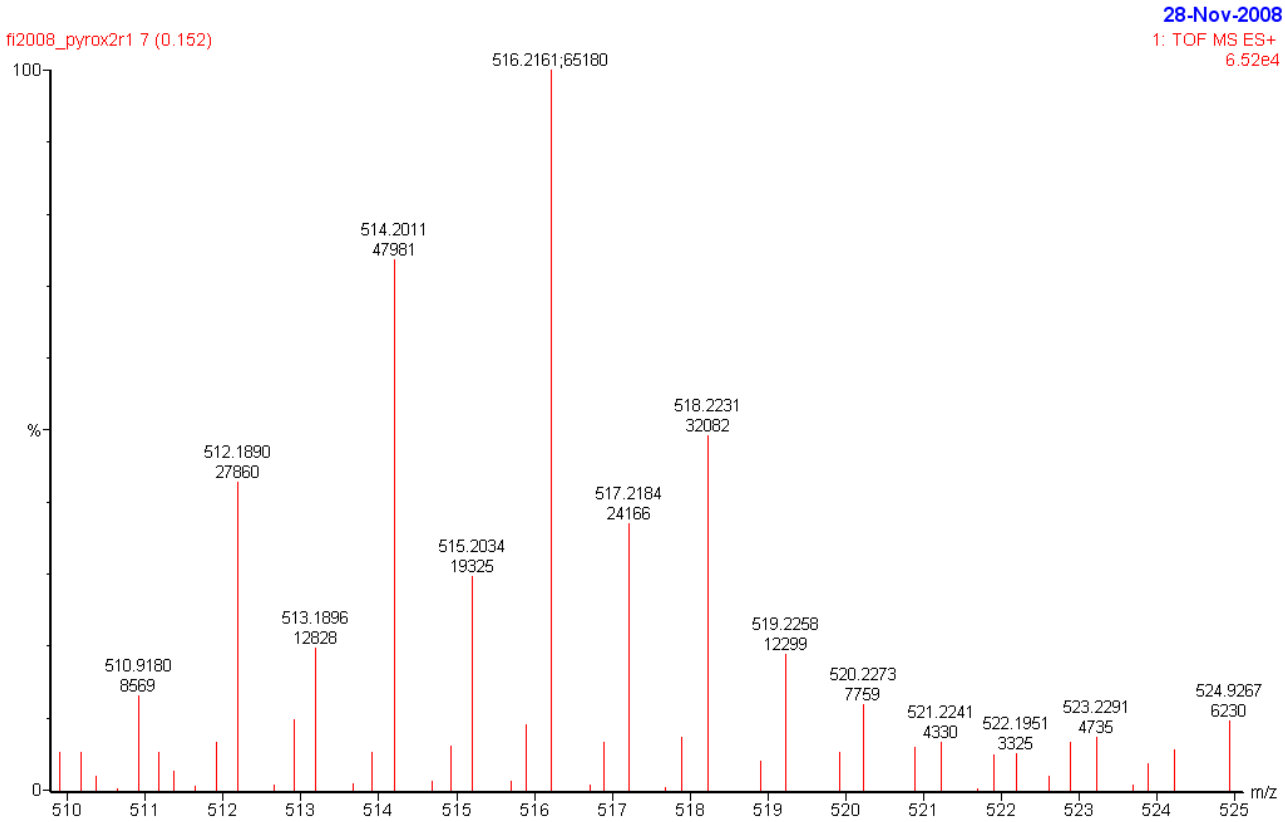

Supp Figure 3: Positive ion high resolution electrospray mass spectrum revealing presence of imnoquinone in pulse radiolysed sample.